Magnetic susceptibility mapping of roadside pollution in the Banaras Hindu University campus, Varanasi, India

Sayandeep Banerjee*, Ankit Kumar, Virendra Rana, Sayan Maity and Hari B. Srivastava

Laboratory for Analysis of Magnetic and Petrofabric, Centre of Advanced Study in Geology, Banaras Hindu University, Varanasi 221 005, India

Among the several methods to determine anthropogenic pollutants in the soil, magnetic susceptibility measurements have proven to be useful for rapid and effective diagnosis of magnetic particles and overall screening of pollution. Magnetic particles and other heavy metals accumulated in the topsoil as a result of roadside pollution, contribute to the bulk magnetic susceptibility (χ). Thus, χ values of the soil can be utilized as a proxy to delineate the zones of high and low roadside pollution in an area. In this study, magnetic susceptibility measurements of the topsoil have been carried out and a quantitative assessment of roadside pollution in the Banaras Hindu University (BHU) campus, Varanasi, India is presented. Based on the χ values of 212 soil samples covering 1300 acres of the campus, zones of high and low roadside pollution are demarcated. The present study has not only deciphered the spatial variation of pollutants in the BHU campus, but has also characterized the magnetic phases responsible for the susceptibility signal on the roadsides inside the campus. The obtained results are crucial for environmental monitoring and prioritization of land use and other anthropogenic activities inside the BHU campus. The *modus operandi* adopted here would be beneficial for mapping areas exposed to different levels of pollution intensity, for tracing the pollution transport and can be effectively applied to various ecosystems.

Keywords: Anthropogenic pollutants, environmental magnetism, magnetic susceptibility, roadside pollution, topsoil.

THE fresh topsoil in an area might get contaminated due to the settling and mixing of air pollutants by anthropogenic activities, and act as a natural storage for the pollutants largely responsible for air pollution. The major contributing factors for increase in the concentration of air pollutants include combustion of fossil fuel resulting in the emission of heavy metals, abrasion/corrosion of asphalt road, construction works and aerosol particles from dust related to urbanization activities[1–4]. Due to the recurrence of such processes, the concentration of toxic pollutants in the topsoil gets enhanced as a result of the settlement and/or accumulation of pollutants alongside roads in urban areas. Apart from the direct and damaging effects of air pollution leading to respiratory problems, these pollutants can also enter the food chain may lead to various health hazards. Therefore, assessment of roadside pollution might help in the prioritization and environmental management of an area to limit/mitigate the effects of accumulating air pollutants in the topsoil. To assess the soil pollutants, various methods have been adopted primarily based on chemical and biochemical analysis[5–10]. However, these methods are often prolonged, arduous and expensive. Alternatively, magnetic methods can be effective in determining heavy metals and other organic pollutants such as polycyclic aromatic hydrocarbons (PAHs) in the soil, efficiently and rapidly[11–13]. Studies have shown that the accumulation of anthropogenic ferrimagnetic and ferromagnetic particles results in a significant enhancement of magnetic susceptibility of soils and dusts, and could be used for the assessment of emission input[14]. It is also suggested that the magnetic susceptibility of the soil is proportional to the concentration of ferrimagnetic minerals such as iron oxides, e.g. magnetite[15]. Nevertheless, the contribution of paramagnetic minerals such as iron-bearing silicates in magnetic susceptibility cannot be neglected[15]. It should also be taken into consideration that the magnetic susceptibility of the soil might be reduced due to the diamagnetic effect of water, carbon, calcium carbonate and silica content[16]. The correlation between concentration of metallic pollutants (mainly Zn, Cd and Cr) and magnetic parameters has also been demonstrated earlier[15,17]. Previous workers have established that measuring the magnetic susceptibility of the soil could be used as a proxy to identify regions with high concentration of magnetic particles, fly ash and other anthropogenic dusts in soils or sediments[11,13,17–23] and thus, can be essentially employed for mapping the roadside pollution of an area. Additionally, it has been argued by several authors that the morphology of magnetic materials provides critical insight into the processes, e.g.

*For correspondence. (e-mail: sayandeep87.geo@bhu.ac.in)

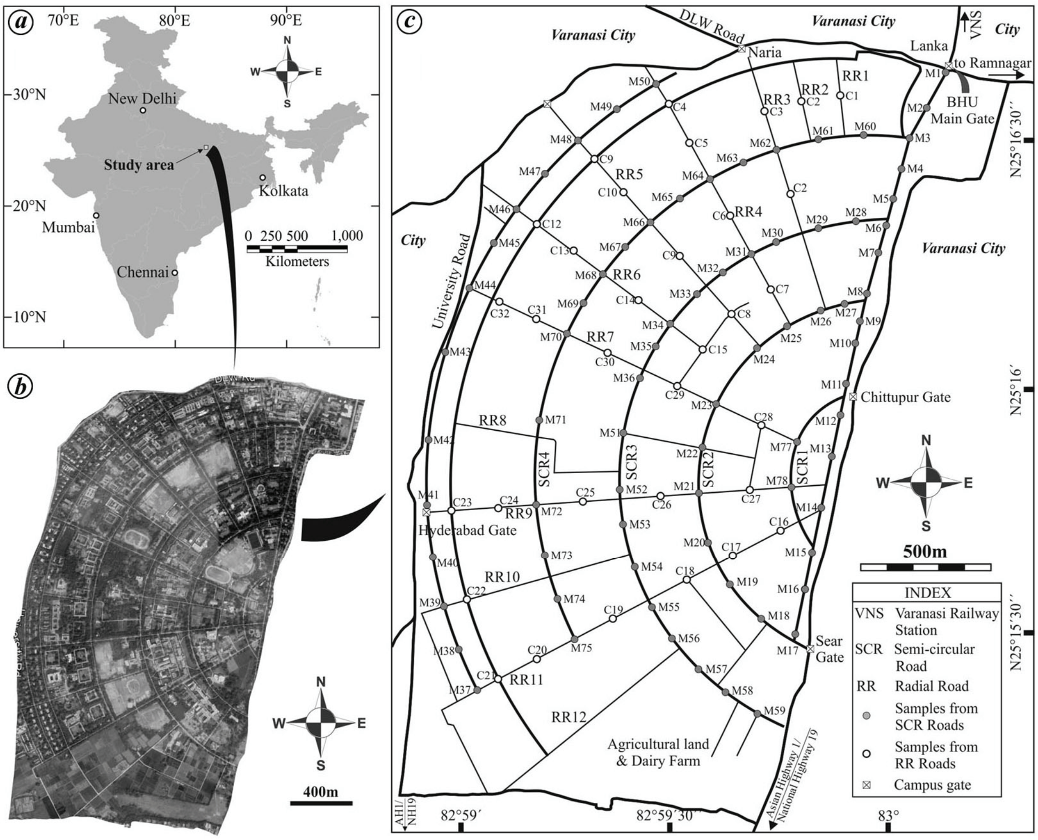

Figure 1. ***a***, Map of India showing the location of Varanasi in Uttar Pradesh. ***b***, Google Earth image of Banaras Hindu University (BHU) main campus in Varanasi. ***c***, Road map of BHU main campus with location of soil samples collected from the main roads (SCR) and connecting roads (RR) inside the campus of 1300 acres (5.3 sq. km) area.

angular-shaped fragments are derived from vehicular emission, dispersion of road construction materials and abrasion of tyres, brake linings and road surfaces, whereas spherical or rounded magnetic particles are possibly a result of industrial and domestic heating systems[24–27]. Earlier it had been considered that the method of magnetic mapping of deposited air–borne particulates of anthropogenic origin from the topsoil is fast, cheap and enables acquisition of large datasets[19]. In this study, we have successfully mapped the roadside pollution in the Banaras Hindu University (BHU) main campus in Varanasi, Uttar Pradesh, India, a more than 100-year old institution of national importance, based on magnetic susceptibility measurements.

Study area

The BHU, established in 1916 by Bharat Ratna Pandit Madan Mohan Malviya, is situated in the southern fringe of Varanasi city at the western bank of River Ganga, and covers an area of ~1300 acres (Figure 1 *a* and *b*). Located at an elevation of 76 m amsl, the climate of the area is humid subtropical with large variations between summer and winter temperatures and annual rainfall of ~982 mm. The alluvial-type soil inside the campus is formed by the deposition of sediments from River Ganga and is fertile, exhibiting sandy loam texture with sand and silt as the dominant constituents of the soil along with clay and soil moisture[28]. According to a recent database, about 30,000 students are enrolled in BHU across 7 institutes and 16 faculties (streams) and about 140 departments. Apart from the 76 hostels occupied by students, a few thousand faculty members and staff members across disciplines reside with their families in several residential colonies and flats, and guest houses in the BHU campus, making it a township with a population of more than 50,000 people. A wide variety of flora[29] and fauna[30] also contribute to the campus ecosystem. Thus, regular environmental monitoring and assessment is necessary for the campus which regulates the livelihood of several thousand people and also helps in the growth of the campus ecosystem.

While a few earlier workers have demonstrated that the BHU campus shows distinctly lower concentration of air pollutants in comparison to the surrounding area of Varanasi city[31], according to a recent report of the Central Pollution Control Board, Ministry of Environment and Forests, Government of India, the Varanasi–Mirzapur industrial cluster is categorized under critically polluted region based on the Comprehensive Environmental Pollution Index (CEPI) score of 85.35 in 2018. Therefore, it

Figure 2. ***a***, Detailed map of BHU main campus depicting the land use inside the campus. Indexing of the land use is provided for effective correlation of the contour maps with the land use inside the campus. The grey area marked in the map is not considered in the present study as the Trauma Centre and Super Specialities Institute (TCSS) was established recently in 2015 and is outside the main campus area. Bulk magnetic susceptibility (χ) contour maps for frequencies at (***b*** and ***c***) 976, (***d*** and ***e***) 3,904 and (***f*** and ***g***) 15,616 Hz, based on soil samples collected during pre-monsoon and post-monsoon months respectively, along the roads at each location shown in Figure 1. The measurement of bulk magnetic susceptibility of each sample was carried out using MFK2-FA kappabridge (see inset) location of the instrument is also shown in (***a***) with a star. (***h***) Rose diagram depicting the dominant wind directions round the year in Varanasi with significant peaks in the wind directions from North and East during winter, and West during summer months.

has become imperative to employ both interdisciplinary and multidisciplinary approaches to monitor and maintain the environment of the BHU campus, an Institute of Eminence (IoE), fostering the holistic development of future generations in consensus with the vision of Mahamana Pandit Madan Mohan Malviya. So the objective of the present study is mainly threefold: (i) to map the roadside pollution of the BHU campus from the accumulation of magnetic pollutants in the soil along the roadside; (ii) to delineate and interpret the plausible reasons for the dispersion of high and low zones of roadside pollution inside the BHU campus and (iii) to identify the heavy minerals/metals present in the soil within the campus.

Materials and method

In view of the mapping of roadside pollution in the BHU campus, 106 locations were selected consisting of 75 along the semi-circular, crescent-shaped roads which are designated as the main traffic roads within the campus, and 31 along the radial roads which connect the semi-circular roads at various places across the campus using a GPS device (Garmin 010 64s) for accuracy (Figure 1 *c*). The locations were selected with ~200–250 m distance between each of them so as to cover all the roads, except the agricultural and farmland present in the southern periphery of the campus, where usual traffic is absent (Figure 1 *c*). A total of 212 samples (each of 40 cm^3 by volume) of the topsoil (0–5 cm) were collected during pre-monsoon (106) and post-monsoon (106) seasons from the predetermined locations to estimate the variation in roadside pollution round the year. Apart from the soil samples, a few leaf samples from the trees along the roadside in the same locations were also taken.

All the soil, dust and leaf samples were collected in air-tight containers during sampling, and later kept in vacuum desiccators in the laboratory to remove air and moisture trapped inside. Subsequently, the dried soil samples were analysed to record the bulk magnetic susceptibility (χ) using MFK2-FA (multifunction kappabridge 2) in the Laboratory for Analysis of Magnetic and Petrofabric (LAMP), Centre of Advanced Study in Geology, BHU (Figure 2). The AGICO-made MFK2-FA kappabridge is the most sensitive (sensitivity: 2×10^{-8} SI) commercially accessible laboratory instrument for measuring the magnetic susceptibility and anisotropy of magnetic susceptibility. MFK2-FA kappabridge permits the measurement of magnetic susceptibility of soils/rocks/liquids at three different frequencies, i.e. 976, 3,904 and 15,616 Hz (ref. 32). The magnetic field is set to 200 A/m. A detailed description of the steps followed during the measurement of χ values using MFK2-FA is provided in the LAMP–BHU protocol developed in the same laboratory[33], and is not discussed here. The soil samples collected during pre-monsoon and post-monsoon seasons were analysed separately and bulk magnetic susceptibility measurement of each sample was carried out following the above methodology. The analysed samples were interpolated by geostatistical method of kriging using Surfer 10 software package. A set of contour maps was prepared to represent the variation in χ values across the campus both spatially and seasonally at three different magnetic frequencies.

To identify the heavy minerals/metals present in the soil, dust and leaf samples, scanning electron microscopy (SEM) was used on selected soil and leaf samples in the Subcontinental Lithospheric Mantle Laboratory, Centre of Advanced Study in Geology, BHU. For SEM analysis, the soil samples were chosen based on the χ values depicting high magnetic susceptibility. Subsequently, the soil samples were dried in vacuum desiccators before SEM analysis. While for the leaf samples, pieces of 2 cm^2 (face and back of the leaves) were prepared and dried before sputtering[34]. The soil, dust and leaf samples were analysed under SEM using back-scattered electrons (BSEs) over carbon-coated sample surface with a working distance of 8 mm and electron high tension of 20 kV. Subsequently, energy-dispersive X-ray spectroscopic (EDS) analysis was performed on selected phases for a semi-quantitative chemical analysis to confirm the heavy mineral phases present in the soil and leaf samples.

Results and discussion

For mapping the roadside pollution of the BHU campus, a map of the study area (scale 1 : 10,000) was prepared depicting the land use inside the campus for effective correlation (Figure 2 *a*). Following the bulk magnetic susceptibility measurements of all the soil samples at varying frequencies (Supplementary Table 1), belonging to pre-monsoon and post-monsoon months, contour maps were prepared based on the χ values of the soil samples (Figure 2 *b*–*g*). The contour maps portray the spatial distribution of high and low zones of bulk magnetic susceptibility across the campus. The influence of wind direction was also evaluated based on the variation of χ values in pre-monsoon and post-monsoon months (Figure 2 *h*). For identification of the exact locations of low–high content of pollutants in the topsoil, Figure 3 *a* and *b* presents a comparative assessment of all samples from the semi-circular roads and radial roads with respect to the χ values.

Zones of high magnetic susceptibility

Significant increase in the χ values (zones of high magnetic susceptibility) was observed near the area around BHU Main Gate, Sir Sundarlal Hospital, Shri Vishwanath Temple, areas around Kendriya Vidyalaya BHU near the Nariya Gate, approach road to Sear Gate (SCR2), adjacent region to the Hyderabad Gate and the SCR3 road connecting the Shri Vishwanath Temple and IIT BHU

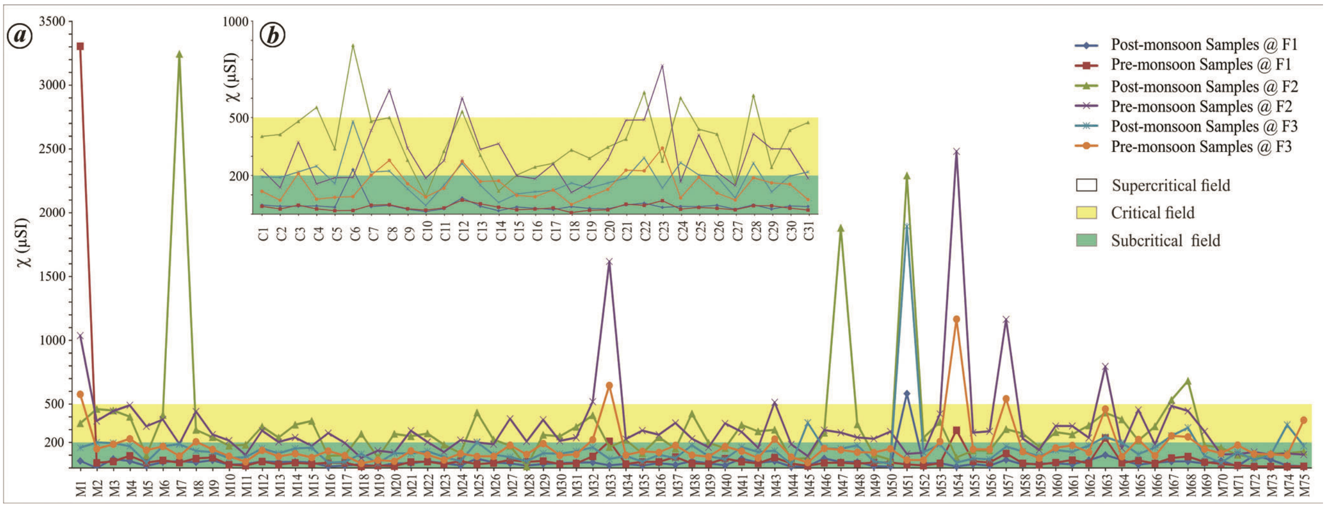

Figure 3. Graph depicting variation in the bulk magnetic susceptibility (χ) values at different frequencies for soil samples (***a***) semi-circular roads (M1–M75) and (***b***) radial roads (C1–C31) inside the BHU campus, as shown in Figure 1 *c*. The supercritical, critical and subcritical fields represent the low, moderate and high content of pollutants in the topsoil respectively. Locations showing χ values below 200 μSI are categorized as permissible, those with χ values in the range 200–500 μSI are categorized under 'alarming situation' and locations with χ values >500 μSI need immediate remedial measures.

entrance (Figures 1 *c*, 2 *a* and 3 *a*). Although significant peaks in the χ values measured during the pre-monsoon and post-monsoon months were comparable (Figure 2 *b*–*g*), a few regions within the campus showed distinct changes during summer compared to the winter months. For instance, a notable upsurge in the bulk magnetic susceptibility was observed in the area around Shri Vishwanath Temple during the post-monsoon months (Figures 2 *b*, *d*, *f* and 3 *a*), but during the pre-monsoon months the χ values were considerably low in the same region (Figures 2 *c*, *e*, *g* and 3 *a*). The semi-circular road (SCR4 in Figure 1 *c*) which connects almost all the hostels in the BHU campus (Figure 2 *a*) also showed a rise in χ values (Figure 2 *b*–*g*), with notable peaks near Ruia, Broacha, Dalmia and Iyer hostels on the SCR4 road (Figures 1 *c*, 2 *a* and 3 *a*). Several high zones of bulk magnetic susceptibility were also observed along the radial roads, e.g. Faculty of Social Science, Premchand Auditorium, Srivastava Canteen, Ashok Park and IIT guest house, among others (Figures 1 *c*, 2 *a* and 3 *b*).

The plausible reason for the high χ values near the BHU main gate is high traffic round the year resulting in the emission of products related to combustion of fossil fuels from the vehicles. The area 'Lanka' outside the BHU Main Gate (Figure 2 *a*) connects it to the rest of Varanasi city (Figure 2 *a*). It is densely populated and a hub for varying anthropogenic activities, leading to an increase in the amount of air pollutants (Figure 2 *b*–*g*). Recent construction works and movement of heavy vehicles in excess near the Nariya Gate for infrastructural development of a cancer hospital in the campus could be responsible for increase in the pollutants in the topsoil, resulting in the high χ values near this region (Figure 2 *a*–*g*). Both Hyderabad Gate and Sear Gate (Figure 1 *c*), leading to the Asian or National Highway (AH1/NH19), are the two busiest locations after the BHU Main Gate, where the movement of a large number of vehicles can be observed throughout the year. This could be responsible for the rise in χ values in regions adjacent to these gates in the campus (Figure 2 *a*–*g*). Being a religious centre (Shri Vishwanath Temple), the temple premise, its surrounding area with cafeterias and its close proximity to the Central Library (Figure 2 *a*), this area also experiences high frequency of vehicular movement and anthropogenic activities leading to an accumulation of heavy mineral/metals in the soil (Figures 2 *b*–*g* and 3 *a*). Especially, in the winter season the temple premise transforms into a tourist spot and attracts several thousands of people every day, leading to an upsurge in the χ values during post-monsoon months relative to the pre-monsoon months (Figures 2 *b*–*g* and 3 *a*). The SCR4 road (Figure 1 *c*) connecting the hostels is also categorized under the zones of high magnetic susceptibility as majority of the students in BHU access this road for their regular entrance and exit from the campus and other activities (Figures 2 *a*–*g* and 3 *a*). Though the detected χ values for the semi-circular roads, largely due to traffic, are considerably higher with respect to the connecting roads, significant peaks are also observed along the radial roads owing to local traffic, and anthropogenic activities concentrated at certain locations (Figure 3 *a* and *b*). The University campus has a road length of ~30 km (Figure 1 *c*), and so even for local transport in the campus different vehicles are being used by students and staff members.

Zones of low magnetic susceptibility

The zones of low magnetic susceptibility are also observed at several locations in the campus depicting a decline

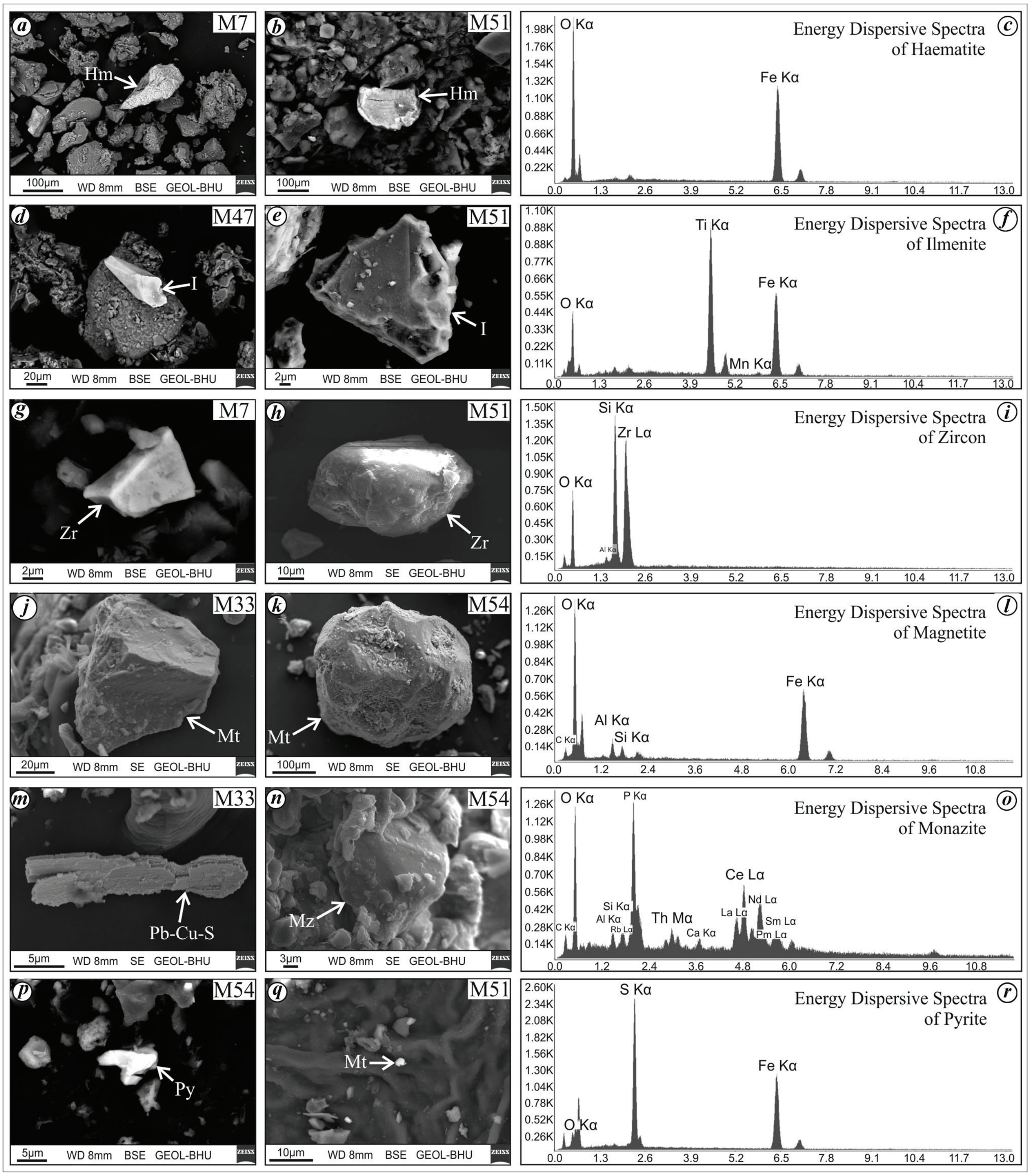

Figure 4. Secondary electron and back-scattered electron microscope images and the respective energy-dispersive X-ray spectroscopic (EDS) spectra of soil, dust and leaf samples alongside the semi-circular roads as shown in Figure 1, inside the BHU main campus. ***a–f***, Sub-angular to sub-rounded fragments of haematite (Hm) and ilmenite (I) occur as bright phases surrounded by quartz and feldspar particles. The mineralogy of the phases is determined through SEM-based EDS spectra. ***g–i***, A few fine-grained euhedral zircons (Zr) are also present in the soil samples as confirmed from the EDS spectra. The zircon grains occur both as angular-shaped and near-spherical particles. ***j*** and ***k***, Presence of bright mineral phases represented by magnetite (Mt). Both sub-angular and spheric-shaped fragments of magnetite can be recognized. ***l***, EDS spectra confirm the occurrence of magnetite in the soil samples. ***m***, Flaky habit of fragments composed of Pb–Cu sulphide and (***n***) sub-rounded grains of monazite (Mz) in the dust samples. ***o***, EDS spectra of monazite in dust samples. ***p–q***, Pyrite (Py) and magnetite (Mt) particles present in the leaf sample of *Tectona grandis* and *Syzygium cumini* respectively, acquired along the roadside. (***r***) EDS spectra confirm the presence of pyrite in the leaves. The locations of soil, dust and leaf samples are provided in the top right corner of each SE or BSE image.

in the accumulation of pollutants in the topsoil. Significantly low χ values are observed near Chittupur Gate, University Club, inside the IIT BHU sector, beside Shri Vishwanath Temple (western rear side), near Madhuban and Botanical Garden (Figure 2 *a*). These locations show distinct fall in the value of bulk magnetic susceptibility, and can be interpreted as the reduced effect of anthropogenic activities and a greater number of trees in this region (Figures 2 *b*–*g* and 3 *a*). Another area showing low χ values is the agricultural land adjacent to the BHU Central Office (Figure 2 *a*); however, its surrounding regions show a rise in the χ values, possibly due to the presence of the Central Library and Academic Staff College on one side and Shri Vishwanath Temple on the other, as discussed above. The southwestern–southern fringe of the University campus, which includes Agricultural Farm, Dairy Farm and Airstrip, shows minimum χ values both during pre-monsoon and post-monsoon months. This zone experiences less frequent movement of vehicles and is mostly restricted, resulting in lower magnetic susceptibility in the vicinity of this whole area. Along the radial roads, significantly low χ values are also observed in front of Bhabha Hostel, Jammu and Kashmir Badminton Hall and IIT Cafeteria (Figure 2 *a*–*g*).

It is interesting to note that the χ values of the collected topsoil during the pre-monsoon months are higher compared to those of collected topsoil measured during the post-monsoon months (Figure 3 *a* and *b*). The increase in the amount of heavy minerals/metals during pre-monsoon season is possibly responsible for this variation. It is also observed that the zones of high magnetic susceptibility during pre-monsoon are more concentrated to the eastern half of the campus (Figures 2 *b*, *d* and *f*). This variation in the magnetic susceptibility could be linked with strong westerly winds during pre-monsoon months in the region (Figure 2 *h*), which might have been responsible in transporting the pollutants and/or heavy minerals more to the eastern part of the campus. However, similar signatures of low and high magnetic susceptibilities across the campus are also recorded in all the three frequencies of measurement, and during both pre-monsoon and post-monsoon seasons. Additionally, it is observed that the χ values measured at F2 frequency (3,904 Hz) give better results compared to F1 (976 Hz) and F3 (15,616 Hz) frequencies. In F2 frequency, the χ values show distinct seasonal variation for samples belonging to pre-monsoon and post-monsoon seasons, whereas in case of F1 and F3 the seasonal variation is often indistinguishable and cannot be relied upon completely (Figure 3 *a* and *b*).

SEM and EDS analysis

For the identification of heavy minerals present as pollutants in the soil, a few soil samples were studied under SEM. BSE images showed the presence of sub-angular to sub-rounded fragments of haematite, with size ranging from ~100 to 300 μm, occurring as bright phases surrounded by quartz and feldspar particles (Figure 4 *a* and *b*). The mineralogy was also confirmed from EDS analysis (Figure 4 *c*). The presence of sub-angular fragments of ilmenite in the soil was also recognized with grain size ranging from ~40 to 100 μm (Figure 4 *d*–*f*). Apart from iron and titanium oxides, very fine-grained zircon (~5–10 μm) was also observed in the soil, and confirmed using EDS analysis (Figure 4 *g*–*i*). SEM images confirmed the presence of both fine-grained (<100 μm) and angular to sub-angular-shaped grains of magnetite in the soil samples along with a few coarse-grained (>100 μm) spherical magnetite fragments (Figure 4 *j*–*l*). Although magnetite is the principal ferromagnetic mineral on earth[35] and occurs as primary or secondary mineral in the continental and oceanic crusts in a range of igneous, sedimentary and metamorphic rocks, the primary source of these magnetic minerals in the urban soils is high-temperature fossil-fuel combustion and related anthropogenic activities[36]. It is to be noted that both angular to sub-angular and rounded to spherical magnetite, haematite, ilmenite and zircon grains are present in the soil samples, which signifies that the anthropogenically produced magnetic particles (APMs) are derived either from traffic emission and natural background input or fossil-fuel combustion. The angular-shaped APMs are usually considered to have originated from vehicular emission, dispersion of road construction materials and abrasion of tyres, brake linings and road surface, whereas the spherical or rounded APMs are a consequence of industrial and domestic heating systems[27]. On the contrary, the cubic shape of magnetic grains is usually retained in case it is derived naturally from the source rock and thus, easily distinguishable from the magnetite grains of anthropogenic origin[27]. Although the soil samples were mainly analysed under SEM to understand the contribution of any heavy/magnetic mineral in the enhancement of χ values of soil at places, a few dust and leaf samples from trees (*Syzygium cumini*, *Tectona grandis*) along the roadside were also analysed. Similar to the soil samples, the dust samples revealed the presence of APMs along with potentially toxic elements (PTEs). The SEM images coupled with EDS spectra confirmed the occurrence of Pb–Cu sulphides and monazite grains (Figure 4 *m*–*o*). The PTEs (e.g. Pb, Cd and Zn) can enter the crystal lattice space of APMs during high-temperature fossil-fuel combustion and might get transported in the down-wind direction[37]. Additionally, the presence of radioactive minerals like monazite contributes significantly to the toxicity levels.

The leaf samples also revealed the presence of heavy minerals, exhibited by brighter phases under BSE mode of SEM, like magnetite, ilmenite and pyrite (Figure 4 *p*–*r*). Apart from AFMs, the ultrafine nature of the magnetite and pyrite grains (<5 μm) poses a greater threat to human lives as these ultrafine particles can enter the human body through various ways and may lead to respiratory, cardiovascular and neurodegenerative diseases[11,38–43].

Substantial evidences are also available testifying that there is a prominent relation between the magnetic susceptibility of sediment, soil and dust samples, and APMs and PTEs[26,44–48]. The occurrence of magnetic phases in soil and leaf is further corroborated with the high magnetic susceptibility of the topsoil inside the campus, which depicts that the χ values for soil samples are significantly higher in case of the topsoil having traces of AFMs as determined from the SEM analysis. It has also been envisaged by earlier workers that the presence of magnetite and haematite in the soil will enhance the χ values in the order of 500–1000 μSI (ref. 17). Thus a combination of environmental magnetism and SEM-based analysis has proved to be useful in the preparation of roadside pollution map of the BHU campus.

Summary

Assessing the contribution of heavy metals/minerals in soil and sediment pollution has become imperative over the last few decades due to the increasing content of industrial pollutants and other atmospheric aerosols. Additional contribution from vehicular emissions and infrastructural activities is responsible for magnetic pollutants in the soil[49]. Earlier studies have demonstrated the correlation between magnetic susceptibility measurements and mutagenic characteristics of atmospheric pollutants with grain size ≤10 μm (ref. 50). It has also been proposed by earlier workers that spherical or rounded particles of anthropogenic origin containing iron oxide-like phases are responsible for the enhancement of magnetic signal in the soil[12] and that magnetite is the principal magnetic mineral for the enhancement of magnetic susceptibility[13]. Primarily, fossil-fuel combustion is responsible for the emission of selected heavy metals and several magnetic particles to the environment[3]. Since the introduction of lead-free petrol, the Pb output is decreasing; however, other heavy metals, including PGE group elements are being emitted in the environment during combustion with many unknown consequences[51,52]. Nevertheless, earlier and present studies show that magnetic methods are inexpensive and effective in the diagnosis of magnetic particles and overall pollution screening.

Determination of heavy metals and magnetic pollutants is crucial because potentially harmful heavy metals can be absorbed in the human body through inhalation ingestion, and dermal contact because of the small size of the heavy metal particles (<10 μm)[42,53,54]. Furthermore, the ultrafine particles (<2.5 μm) may pass through the lungs and reach the blood circulation, and also into the extra-pulmonary tissues and organs resulting in severe damage from dosimetric effects. It should be noted that the micrometre-sized magnetic iron oxides may induce oxidative stress pathways, which leads to the formation of free radicals, and might cause DNA damage[11,43,55]. It has also been reported that ultrafine micrometre to nanometre-sized airborne magnetic particles can enter the human brain and damage the reactive oxygen species leading to neurodegenerative diseases such as Alzheimer's disease[41]. The principal source of this micrometre to nanometre-sized magnetic particles is the iron impurities in the fossil fuel, which convert to magnetic iron oxides during combustion, i.e. magnetite, hematite, maghemite or a mixture, depending on the combustion conditions[56]. Thus, recognition of the zones with high content of airborne magnetic particles is essential for prioritization of human activities. This can be accomplished by a combination of magnetic susceptibility and electron microscopic studies of roadside soil and/or dust.

The present study has not only deciphered the spatial variation of pollutants in the BHU campus, but has also characterized the magnetic phases responsible for the susceptibility signal on the roadsides inside the campus (Figures 2 *b–g*, 3 and 4). Other factors such as change in the wind direction of the Varanasi area annually are perhaps responsible for the spatial variation in the zones of high and low roadside pollution during pre-monsoon and post-monsoon months (Figure 2 *h*). Based on the χ values, a broad classification depicting the zonation of low and high accumulation of air pollutants is also suggested (Figure 3). It has been reported earlier that magnetic susceptibility values are >500 μSI for soils/rocks having high content of ferromagnetic minerals[57]. On the contrary, magnetic susceptibility values between 0 and 200 μSI are considered to be the result of paramagnetic minerals and accordingly, magnetic susceptibility values between 200 and 500 μSI are possibly due to a mixture of paramagnetic and ferromagnetic minerals in the soil. Based on this categorization, soil samples showing magnetic susceptibility values >500, 200–500 and <200 μSI are classified under supercritical, critical and subcritical fields respectively (Figure 3). Therefore, the locations with χ values of 200–500 μSI are categorized under alarming situation, and those with χ values >500 μSI need immediate remedial measures, while locations with χ values <200 μSI are not under immediate threat but need intermittent monitoring.

It is also observed that bulk magnetic susceptibility measurements carried out at F2 frequency provide better results in terms of variation among pre-monsoon and post-monsoon samples compared to F1 and F3 frequencies. However, the background reason for this variation could not be explained in the present study. This requires further research based on the relationship between measurement frequencies and magnetic mineralogy of the soil samples.

Conclusion

This study presents the first quantitative assessment of roadside pollution in the BHU main campus, since its establishment in 1916 in Varanasi. The salient outcomes of the study are listed below.

(a) It is demonstrated that the bulk magnetic susceptibility measurements of the topsoil can be rapidly used as a proxy to delineate the zones of high and low roadside pollution in an area.

(b) The spatial distribution of the zones of high and low roadside pollution is controlled by the emission of selected heavy metals due to fuel combustion and/or construction works related to infrastructural development inside the BHU campus.

(c) SEM and EDS analyses confirm the occurrence of heavy minerals like magnetite, haematite, ilmenite, zircon, pyrite, etc. in the topsoil of the BHU campus.

(d) The results of the present study could be applied for environmental monitoring and prioritization of land use and other anthropogenic activities inside the BHU campus.

(e) It is suggested that roadside plantation of deciduous trees and improvement in the drainage system within the campus are essential to reduce the accumulation of pollutants in the topsoil near the sites of infrastructural development and busy campus roads, resulting in a smaller stay time of the heavy metals in the topsoil, roadside dust and tree leaves.

(f) The *modus operandi* adopted here could be replicated to assess the roadside pollution, for mapping areas exposed to different levels of pollution intensity, for tracing the pollution transport and can be effectively applied to various ecosystems for monitoring and mitigation.

1. Gadi, R. *et al.*, Mass size distribution and chemical composition of aerosols at New Delhi. In *Environment Pollution* (eds Siddappa, K. *et al.*), Bangalore University, Bengaluru, 2000, vol. 30–32.
2. Mönkkönen, P. *et al.*, Relationship and variations of aerosol number and PM10 mass concentrations in a highly polluted urban environment – New Delhi, India. *Atmos. Environ.*, 2004, **38**, 425–433.
3. Wang, T. *et al.*, Chemical characterization of the boundary layer outflow of air pollution to Hong Kong during February–April 2001. *J. Geophys. Res. Atmos.*, 2003, **108**, **B2**, 1–21.
4. Yadav, S. and Rajamani, V., Air quality and trace metal chemistry of different size fractions of aerosols in N–NW India – implications for source diversity. *Atmos. Environ.*, 2006, **40**, 698–712.
5. Chen, T. *et al.*, Assessment of trace metal distribution and contamination in surface soils of Hong Kong. *Environ. Pollut.*, 1997, **96**, 61–68.
6. Häni, H., The analysis of inorganic and organic pollutants in soil with special regard to their bioavailability. *Int. J. Environ. Anal. Chem.*, 1990, **39**, 197–208.
7. Jia, Z., Li, S. and Wang, L., Assessment of soil heavy metals for eco-environment and human health in a rapidly urbanization area of the upper Yangtze Basin. *Sci. Rep.*, 2018, **8**, 1–14.
8. Luo, L. *et al.*, Relationships between aging of PAHs and soil properties. *Environ. Pollut.*, 2012, **170**, 177–182.
9. Pan, L., Yao, E. and Yang, Y., Impact analysis of traffic-related air pollution based on real-time traffic and basic meteorological information. *J. Environ. Manage.*, 2016, **183**, 510–520.
10. Samara, C. and Voutsa, D., Size distribution of airborne particulate matter and associated heavy metals in the roadside environment. *Chemosphere*, 2005, **59**, 1197–1206.
11. Evans, M. and Heller, F., *Environmental Magnetism: Principles and Applications of Enviromagnetics*, Elsevier, San Diego, California, USA, 2003.
12. Flanders, P. J., Collection, measurement, and analysis of airborne magnetic particulates from pollution in the environment. *J. Appl. Phys.*, 1994, **75**, 5931–5936.
13. Hoffmann, V., Knab, M. and Appel, E., Magnetic susceptibility mapping of roadside pollution. *J. Geochem. Explor.*, 1999, **66**, 313–326.
14. Dekkers, M. and Pietersen, H., Magnetic properties of low-Ca fly ash: a rapid tool for Fe-assessment and a survey for potentially hazardous elements. *Mater. Res. Soc. Symp. Proc.*, 1992, **245**, 37–47.
15. Georgeaud, V. *et al.*, Relationship between heavy metals and magnetic properties in a large polluted catchment: the Etang de Berre (South of France). *Phys. Chem. Earth*, 1997, **22**, 211–214.
16. Hunt, A., Jones, J. and Oldfielcl, F., Magnetic measurements and heavy metals in atmospheric particulates of anthropogenic origin. *Sci. Total Environ.*, 1984, **33**, 129–139.
17. Boyko, T. *et al.*, Topsoil magnetic susceptibility mapping as a tool for pollution monitoring: repeatability of *in situ* measurements. *J. Appl. Geophys.*, 2004, **55**, 249–259.
18. Knab, M. *et al.*, Surveying the anthropogenic impact of the Moldau river sediments and nearby soils using magnetic susceptibility. *Environ. Geol.*, 2006, **49**, 527–535.
19. Petrovský, E. and Ellwood, B., Magnetic monitoring of air, land and water pollution. In *Quaternary Climates and Magnetism* (eds Maher, B. and Thompson, R.), Cambridge University Press (CUP), Cambridge, UK, 1999, pp. 279–322.
20. Strzyszcz, Z., Magnetic susceptibility of soils in the areas influenced by industrial emissions. In *Soil Monitoring*, Springer, 1993, pp. 255–269.
21. Strzyszcz, Z. and Magiera, T., Magnetic susceptibility and heavy metals contamination in soils of southern Poland. *Phys. Chem. Earth*, 1998, **23**, 1127–1131.
22. Mondal, S., Chatterjee, S., Maity, R., Gain, D., Das, A. and Sinha, S., Magnetic susceptibility as a proxy for pollution in the Triveni–Bandel area, Hooghly district, West Bengal, India. *Curr. Sci.*, 2017, **112**, 2306–2311.
23. Mondal, S., Chatterjee, S. and Gain, D., Mineralogy and morphological characterization of technogenic magnetic particles (TMP) from industrial dust: insights into environmental implications. In *Spatial Modelling and Assessment of Environmental Contaminants* (eds Shit, P. K., Adhikary, P. P. and Sengupta, D.), Springer, Cham, 2021, pp. 515–529.
24. Banerjee, S. K., King, J. and Marvin, J., A rapid method for magnetic granulometry with applications to environmental studies. *Geophys. Res. Lett.*, 1981, **8**, 333–336.
25. Tissari, J., Lyyränen, J., Hytönen, K., Sippula, O., Tapper, U. and Frey, A., Fine particle and gaseous emissions from normal and smouldering wood combustion in a conventional masonry heater. *Atmos. Environ.*, 2008, **42**, 7862–7873.
26. Bućko, M. S., Magiera, T., Pesonen, L. J. and Janus, B., Magnetic, geochemical, and microstructural characteristics of road dust on roadsides with different traffic volumes – case study from Finland. *Water Air Soil Pollut.*, 2010, **209**, 295–306.
27. Maity, R. *et al.*, Magnetic and microscopic characterization of anthropogenically produced magnetic particles: a proxy for environmental pollution. *Int. J. Environ. Sci. Technol.*, 2021, **18**, 1793–1808.
28. Chaturvedi, R. *et al.*, Effect of dust load on the leaf attributes of the tree species growing along the roadside. *Environ. Monit. Assess.*, 2013, **185**, 383–391.

29. Singh, A., Exotic flora of the Banaras Hindu University main campus. *Indian J. Ecol. Nat. Environ*., 2011, **3**, 337–343.
30. Nayak, A. and Ghosh, S., Moth diversity (Lepidoptera: Heterocera) of Banaras Hindu University, Varanasi, India: a preliminary checklist. *Not. Sci. Biol.*, 2020, **12**, 592–607.
31. Agrawal, M. *et al.*, Effect of air pollution on peri-urban agriculture: a case study. *Environ. Pollut.*, 2003, **126**, 323–329.
32. Chadima, M., Hrouda, F, and V. Jelinek, Anisoft5, 2018.
33. Rana, V., Kumar, P., Banerjee, S. and Biswas, A., Magnetic susceptibility investigation of the saline water intrusion problem – The LAMP-BHU protocol. *J. Earth Syst. Sci.*, 2021, **130**, 1–11.
34. Hanesch, M., Scholger, R. and Rey, D., Mapping dust distribution around an industrial site by measuring magnetic parameters of tree leaves. *Atmos. Environ*., 2003, **37**, 5125–5133.
35. Dunlop, D. J. and Özdemir, Ö., Rock *Magnetism, Fundamentals and Frontiers*, CUP, Cambridge, UK, 1997.
36. Petrovský, E., Alcala, M. D., Criado, J. M., Grygar, T., Kapička, A. and Subrt, J., Magnetic properties of magnetite prepared by ball-milling of hematite with iron. *J. Magn. Magn. Mater.*, 2000, **210**, 257–273.
37. Kapicka, A., Petrovsky, E., Ustjak, S. and Machackova, K., Proxy mapping of fly-ash pollution of soils around a coal burning power plant: a case study in the Czech Republic. *J. Geochem. Explor.*, 1999, **66**, 291–297.
38. Han, X. and Naeher, L. P., A review of traffic-related air pollution exposure assessment studies in the developing world. *Environ. Int.*, 2006, **32**, 106–120.
39. Pope, C. A. and Dockery, D. W., Health effects of fine particulate air pollution: lines that connect. *J. Air. Waste Manage. Assoc*., 2006, **56**, 709–742.
40. Knox, A. S., Paller, M. H., Nelson, E. A., Specht, W. L., Halverson, N. V. and Gladden, J. B., Metal distribution and stability in constructed wetland sediment. *J. Environ. Qual.*, 2006, **35**, 948–959.
41. Maher, B. A. *et al*., Magnetite pollution nanoparticles in the human brain. *Proc. Natl. Acad. Sci. USA*, 2016, **113**, 10797–10801.
42. Bourliva, A., Christophoridis, C., Papadopoulou, L., Giouri, K., Papadopoulos, A., Mitsika, E. and Fytianos, K., Characterization, heavy metal content and health risk assessment of urban road dusts from the historic center of the city of Thessaloniki, Greece. *Environ. Geochem. Health*, 2017, **39**, 611–634.
43. Hoffman, E., Guernsey, J. R., Walker, T. R., Kim, J. S., Sherren, K. and Andreou, P., Pilot study investigating ambient air toxics emissions near a Canadian kraft pulp and paper facility in Pictou County, Nova Scotia. *Environ. Sci. Pollut. Res.*, 2017, **24**, 20685–20698.
44. Jordanova, N. V., Jordanova, D. V., Veneva, L., Yorova, K. and Petrovský, E., Magnetic response of soils and vegetation to heavy metal pollution – a case study. *Environ. Sci. Technol.*, 2003, **37**, 4417–4424.
45. Chaparro, M. A. E., Bidegain, J. C., Sinito, A. M., Jurado, S. S. and Gogorza, C. S. G., Relevant magnetic parameters and heavy metals from relatively polluted stream sediments – vertical and longitudinal distribution along a cross-city stream in Buenos Aires Province, Argentina. *Stud. Geophys. Geod.*, 2004, **48**, 615–636.
46. Maher, B. A., Moore, C. and Matzka, J., Spatial variation in vehicle derived metal pollution identified by magnetic and elemental analysis of roadside tree leaves. *Atmos. Environ.*, 2008, **42**, 364–373.
47. Yang, T., Liu, Q., Zeng, Q. and Chan, L., Relationship between magnetic properties and heavy metals of urban soils with different soil types and environmental settings: implications for magnetic mapping. *Environ. Earth. Sci.*, 2012, **66**, 409–420.
48. Wang, X. S., Mineralogical and chemical composition of magnetic fly ash fraction. *Environ. Earth. Sci.*, 2014, **71**, 1673–1681.
49. Hunt, A., The application of mineral magnetic methods to atmospheric aerosol discrimination. *Phys. Earth Planet. Inter*., 1986, **42**, 10–21.
50. Morris, W. *et al.*, Preliminary comparisons between mutagenicity and magnetic susceptibility of respirable airborne particulate. *Atmos. Environ*., 1995, **29**, 3441–3450.
51. Puchelt, H., Eckhardt, J. and Schaefer, J., Deposition of platinum group elements (PGEs) from motor vehicle exhaust gas catalysts to soil near roads. Eintraege von Platingruppenelementen (PGE) aus Kfz-Abgaskatalysatoren in strassennahe Boeden, Germany, 1995, p. 21.
52. Schäfer, J. and Puchelt, H., Platinum-group-metals (PGM) emitted from automobile catalytic converters and their distribution in roadside soils. *J. Geochem. Explor.*, 1998, **64**, 307–314.
53. Hu, Y., Liu, X., Bai, J., Shih, K., Zeng, E. Y. and Cheng, H., Assessing heavy metal pollution in the surface soils of a region that had undergone three decades of intense industrialization and urbanization. *Environ. Sci. Pollut. Res.*, 2013, **20**, 6150–6159.
54. Xing, W., Zhang, H., Scheckel, K. G. and Li, L., Heavy metal and metalloid concentrations in components of 25 wheat (*Triticum aestivum*) varieties in the vicinity of lead smelters in Henan province. *China Environ. Monit. Assess*., 2016, **188**, 1–10.
55. De, Kok, T. M., Driece, H. A., Hogervorst, J. G. and Briedé, J. J., Toxicological assessment of ambient and traffic-related particulate matter: a review of recent studies. *Mutat. Res. Rev. Mutat. Res*., 2006, **613**, 103–122.
56. Muxworthy, A. R., Schmidbauer, E. and Petersen, N., Magnetic properties and Mossbauer spectra of urban atmospheric particulate matter: a case study from Munich. *Geophys. J. Int.*, 2002, **150**, 558–570.
57. Bouchez, J. L., Granite is never isotropic: an introduction to AMS studies of granitic rocks. In *Granite: from Segregation of Melt to Emplacement Fabrics*, Springer, Dordrecht, 1997, pp. 95–112.

ACKNOWLEDGEMENTS. We thank Prof. B. P. Singh (Head, Department of Geology, Banaras Hindu University (BHU), Varanasi) for providing infrastructural facilities. S.B. and H.B.S. acknowledge financial support provided by DST-PURSE 5050 programme for the procurement of AGICO-made MFK2-FA kappabridge instrument. This study contains data pertaining to the M Sc dissertation of A.K. under the supervision of S.B. We also thank Aman Verma (BHU) for his help during the collection of soil samples; the SCLM laboratory staff members (Department of Geology, BHU), especially, N. V. Chalapathi Rao and Sneha Raghuvangshi for help during SEM analyses. Efficient editorial handling by Prof. Dilip Saha (Indian Statistical Institute, Kolkata) and comments from the anonymous reviewers helped improve the manuscript. V.R. thanks UGC, New Delhi for D. S. Kothari Post-doctoral Fellowship (Ref. No. F.4-2/2006(BSR)/ES/18-19/0003). This study marks the fifth contribution of the Laboratory for Analyses of Magnetic and Petrofabric at BHU.

Received 21 June 2021; accepted 5 August 2021

doi: 10.18520/cs/v121/i8/1046-1055